

## Solubility Behavior and Prediction for Anthelmintics at Several Temperatures in Aqueous and Nonaqueous Mixtures

Pilar BUSTAMANTE,\* Susana MUELA, Begoña ESCALERA, and Ángeles PEÑA

*Departamento de Farmacia y Tecnología Farmacéutica, Facultad de Farmacia, Universidad de Alcalá; Alcalá de Henares, 28871, Madrid, Spain.* Received November 3, 2009; accepted February 22, 2010; published online February 25, 2010

**A model based on solubility parameters is proposed to predict the solubility curves of anthelmintic drugs at several temperatures, including aqueous and non-aqueous mixtures. The solubility of the drugs was measured in ethanol–water and ethanol–ethyl acetate mixtures at 15–35 °C (mebendazole) and at 25 °C (thiabendazole and metronidazole). The solid phases were analyzed by differential scanning calorimetry. The polymorphic form A of mebendazole was also characterized from infrared spectroscopy. Markedly different solubility profile shapes were obtained against the solubility parameter of the mixtures: two symmetrical peaks (metronidazole), two maxima of different height (mebendazole) and a single peak (thiabendazole). The solubility parameter of the drugs was related to the co-solvent action of both mixtures and to the solubility peaks. The single equation proposed was able to predict solubility profiles of different shape, including both mixtures and all temperatures, providing reasonable physical meaning for the regression coefficients. The model was successfully tested for its predictive capability using a limited number of experimental data. More than 100 solubilities were predicted at several temperatures using 20 data point for each drug.**

**Key words** solubility prediction; solubility parameter; anthelmintic drug; solvent mixture; solid phase characterization

Solubility is a fundamental physico-chemical property with important applications to biological, chemical, pharmaceutical and environmental industries. Reliable solubility data require careful experimental measurements that are tedious, time consuming and costly, and this research area needs further investigation.<sup>1)</sup> Solubility data for drugs in solvent mixtures at several temperatures are scarce, in particular in solvent mixtures.<sup>2–7)</sup> These data allow to obtain thermodynamic magnitudes that provide a better understanding of the co-solvent action and solute–solvent interactions.<sup>2–6,8)</sup> Aqueous mixtures are often used to increase the solubility of drugs. Non-aqueous mixtures have application in synthesis, re-crystallization and purification of drugs and in some techniques of microencapsulation.<sup>9,10)</sup> The solubility data also serve to construct mathematical models that help to optimize solvent composition selection in pharmaceutical technology. Many drug candidates are so hydrophobic that its bioavailability depends on techniques to enhance the aqueous solubility.<sup>11)</sup> During the earlier stages of drug development the amount available of drug is often restrictive. Therefore it is desirable to have a model for correlating and predicting drug solubility from a small amount of data being at the same time easy to apply. Solubility prediction is very difficult because it depends on a large number of factors such as chemical structure, solute–solvent interactions and temperature. The drugs usually form non-ideal solutions with the solvents of pharmaceutical interest, and semi-empirical or empirical approaches are often needed to obtain useful solubility prediction. Solubility modelling may significantly reduce the experimental work in solvent selection.

Predictive methods often require a number of physico-chemical parameters and relatively complicate computation, and low prediction capability has been reported for the universal functional group activity coefficient (UNIFAC) method in some compounds.<sup>1)</sup> The log-linear model of Yalkowsky is not applicable for drugs showing a solubility maximum, and a model was developed to account for deviations from linearity in ethanol-water mixtures.<sup>12)</sup> In fact, when solubility behav-

our of drugs is studied within a wide polarity range, curves with one or two solubility peaks may be found.<sup>6)</sup>

Mota *et al.*<sup>11)</sup> used the Non-random Two Liquid Segment Activity Coefficient (NRTL-SAC) model for predicting the solubility in pure solvents and solvent mixtures at 25–40 °C. The model requires the melting data from the solid phase,  $T_f$ ,  $\Delta H_f$  and  $\Delta C_p$ . Limited experimental  $\Delta C_p$  values are available for drugs and this contribution is frequently ignored in solubility calculations.<sup>11)</sup> The predictions did not agree well with the experimental data of paracetamol at high ethanol–in water ratios, a fact that was attributed to the appearance of a peak in the solubility profile, as was earlier reported.<sup>13,14)</sup>

Bustamante and co-workers proposed a model to predict the solubility mole fraction  $\ln X_2$  of drugs showing two solubility peaks in solvent mixtures at a particular temperature.<sup>15,16)</sup> In this work we expand our earlier model to include in a single equation several temperatures and two solvent mixtures (Eq. 1):

$$\ln X_2 = C + C_1\delta_1 + C_2\delta_1^2 + C_3\delta_{1a} + C_4\delta_{1b} + C_5\delta_{1a}\delta_{1b} + T + I \quad (1)$$

$T$  is the temperature,  $\delta_1$  is the Hildebrand solubility parameter,  $\delta_{1a}$  and  $\delta_{1b}$  the acidic and basic partial solubility parameters of Karger *et al.*,<sup>17)</sup> and  $I$  is a variable indicator taking values of  $I=1$  and  $I=0$  for aqueous and non-aqueous mixtures, respectively.

For solvent mixtures, the Hildebrand and partial solubility parameters can be calculated as a linear combination of the  $\delta$ 's of the pure solvents and the volume fraction of the solvents in the mixture.<sup>18)</sup>

The coefficients  $C_0$ – $C_5$  are obtained from multiple linear regression, and the melting temperature and the heat of fusion are not required in the model. For a given drug, these are constant values included into the intercept  $C_0$ . This is advantageous because some drugs decompose during melting and these thermodynamic magnitudes cannot be properly measured.

The terms included into the solubility model may be re-

\* To whom correspondence should be addressed. e-mail: pilar.bustamante@uah.es

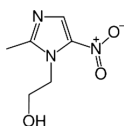


Fig. 1. Chemical Structure of Metronidazole (MTZ)

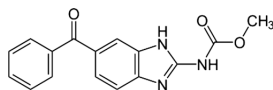


Fig. 2. Chemical Structure of Mebendazole (MBZ)

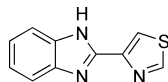


Fig. 3. Chemical Structure of Thiabendazole (TBZ)

lated to several types of interactions. The squared term  $\delta_1^2$  and the product  $\delta_{1a}\delta_{1b}$  account for self-association of the solvent through non-specific and specific interactions that decrease solubility. The linear terms are related to van der Waals ( $\delta_1$ ) and Lewis acidic ( $\delta_{1a}$ ) and basic ( $\delta_{1b}$ ) solute-solvent interactions that increase solubility.

Equation 1 is proposed to predict solubility profiles combining several temperatures and two different solvent mixtures (aqueous and non-aqueous) for drugs showing one or two solubility maxima.

Equation 1 is tested to model the solubility behaviour of three antihelmintic drugs. Mebendazole (MBZ) is a benzimidazole (methyl (6-benzoyl-1*H*-benzimidazol-2-yl) carbamate) of broad spectrum used to treat infestations by worms. Mebendazole may exist as polymorphic forms A, B, and C.<sup>19,20</sup> Metronidazole (MTZ) is a nitroimidazole (methyl 2-(2-methyl-5-nitro-1*H*-imidazol-1-yl) used mainly in the treatment of infections caused by anaerobic bacteria and protozoa. Thiabendazole (TBZ) is a benzimidazole (4-(1*H*-1,3-benzodiazol-2-yl)-1,3-thiazole), used as fungicide and parasiticide (Figs. 1–3).

The experimental solubility of mebendazole (MBZ) was determined at several temperatures (5–35 °C). The solubilities of metronidazole (MTZ) and thiabendazole (TBZ) were determined at 25 °C, and the data at other temperatures can be found elsewhere.<sup>21)</sup>

## Experimental

**Materials** Mebendazole (MBZ), metronidazole (MTZ) and thiabendazole (TBZ) were purchased from Sigma-Aldrich (Steinheim, Germany) (batches 35H0610, 54H0407 and 65H0302; respectively). The solvents used were ethyl acetate, ethanol (spectrophotometric grade; Panreac, Monplet and Esteban, Barcelona, Spain) and double-distilled water.

**Methods. Differential Scanning Calorimetry (DSC)** Samples of about 5 milligrams (mg) were heated in aluminium pans under nitrogen gas purge in a differential scanning calorimeter (Mettler TA 4000, Switzerland). The thermal behaviour of the original powders of the drugs and that of the solid phases after equilibration with the pure solvents were analyzed at 5 °C/min (or 10 °C/min to check differences with heating rate). The solid non-dissolved phases were placed on filter papers and the solvent excess was gently evaporated at room temperature until constant weight. This procedure was chosen because more drastic conditions may remove solvent loosely bound to the crystals that may affect the thermal behaviour of the solid phase.<sup>22)</sup> The experiments were performed in triplicate.

**Fourier Transforms Infrared Spectroscopy (FT-IR)** Fourier transform IR spectra were examined over the scanning range of 650–4000 cm<sup>-1</sup> using

Table 1. Thermal Events for MTZ, MBZ and TBZ before and after Equilibration with Pure Solvents

Drugs	Original powders		Solid phases after equilibration		
	<i>T</i> (°C)	$\Delta H$ (kJ/mol)	Pure solvents	<i>T</i>	$\Delta H$
MTZ	160.8	32.65	Water	160.7	33.51
			Ethanol	160.6	33.50
			Ethyl acetate	160.5	33.90
MBZ <sup>a)</sup>	251.6	77.30	Water	251.7	51.53
				303.2	50.58
	304.0	78.20	Ethanol	256.6	58.72
				305.3	73.00
			Ethyl acetate	257.5	61.67
			306.3	71.00	
TBZ	300.7	35.19	Water	300.7	34.96
			Ethanol	300.6	34.52
			Ethyl acetate	300.2	32.58

a) Two endothermic effects.

a Spectrum 2000 spectrometer (Perkin Elmer, U.S.A.). The resolution was 1 cm<sup>-1</sup>. The spectra were recorded for mebendazole and for the crystals obtained after contact with water, ethanol and ethyl acetate. Samples of 2 mg were mixed with 100 mg of potassium bromide and gently ground in a mortar. The samples were analysed from disks of about 13 mm diameter prepared with KBr and compressed in a hydrostatic press at a force of 5 T for 2 min.

**Solubility Determination** Sealed flasks containing an excess of powder in the pure solvents and solvent mixtures were shaken in a temperature-controlled bath (Heto SH 02/100, Denmark;  $\pm 0.1$  °C). The saturation concentration was determined from the asymptotic regions of the dissolution curves *versus* time. When equilibrium solubility was attained, the solid phase was removed by filtration (Durapore membranes, 0.2  $\mu$ m pore size, Millipore Ibérica S.A., Spain). The drugs did not significantly adsorb onto the membranes. The clear solutions were diluted with ethanol 96% (v/v) and assayed in a double-beam spectrophotometer (Shimadzu UV-2001PC, U.S.A.). The measurements were performed at 247 nm for MBZ, 312 nm for MTZ and 300 nm for TBZ. The densities of the solutions were determined at each temperature in 10-ml pycnometers. All the experimental results are the average of at least three replicated experiments. The coefficient of variation is within 2% among replicated samples for the solubility measurements.

## Results and Discussion

**Solid Phase Characterization** Table 1 summarizes the thermal events before and after equilibration of the drugs with the pure solvents. The peaks of fusion are  $T_f = 160.82$  °C ( $\Delta H_f = 32.65$  kJ/mol) for MTZ and  $T_f = 300.7$  °C ( $\Delta H_f = 35.19$  kJ/mol) for TBZ. The solid phases did not show new thermal effects after equilibration with the solvents, and the temperatures and enthalpies at the peaks are similar to those found for the three original powders.

Mebendazole may exist under three polymorphic forms, A, B and C, and the thermal effects obtained correspond to the most stable and less soluble Form A at room temperature (Fig. 4). The original powder shows an endothermic/exothermic transition ( $T_1 = 251.6$ – $260$  °C,  $\Delta H = 77.33$  kJ/mol) and a second endothermic peak ( $T_2 = 304$  °C,  $\Delta H = 78.23$  kJ/mol) at a heating rate of 5 °C/min. The temperature at the peaks is somewhat higher at 10 °C/min ( $T_1 = 260.75$  °C and  $T_2 = 315.52$  °C, respectively) due to the greater sensitivity and less resolution. De Villiers *et al.*<sup>20)</sup> reported these two effects at 250–255 °C and 330 °C and Himmelreich *et al.*<sup>23)</sup> found two endotherms at 235 °C and 320 °C (heating rate, 10 °C/min).

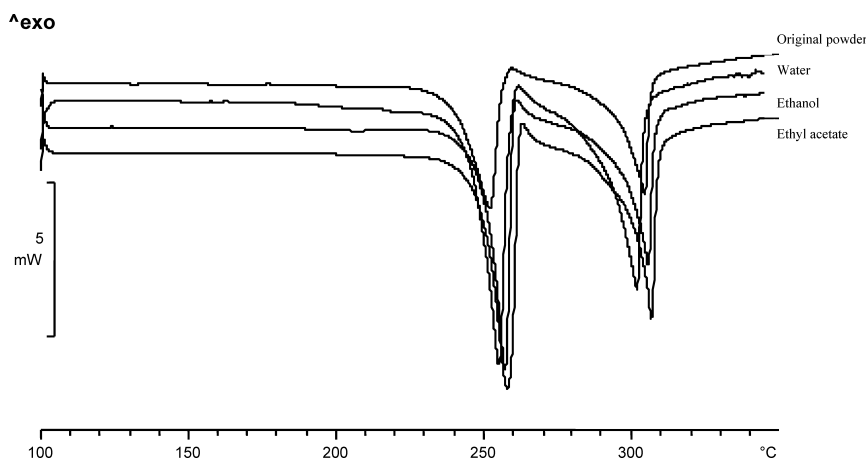


Fig. 4. DSC-Profile of Mebendazole (Original Powder) and of the Solid Phases after Equilibration from the Pure Solvents

Table 2. Principal IR Absorption Peaks ( $\text{cm}^{-1}$ ) and Thermal Events for MBZ Polymorphs

Polymorph	IR ( $\text{cm}^{-1}$ )			$T$ ( $^{\circ}\text{C}$ )
	-NH	CO=	CONH-	
A <sup>a)</sup>	3370	1730	1650	250—330 <sup>c)</sup>
B <sup>a)</sup>	3340	1700		220—263—330 <sup>c)</sup>
C <sup>a)</sup>	3410	1720		195—225—253—330 <sup>c)</sup>
A <sup>b)</sup>	3369	1732	1638	251—304 <sup>b)</sup>

a) Swanepoel *et al.*<sup>24)</sup>; b) this work; c) de Villiers *et al.*<sup>20)</sup>

The thermograms of the mebendazole non-dissolved solid phase after equilibration with water, ethanol and ethyl acetate did not show new thermal events (Fig. 4) suggesting that the solvents do not induce solid phase changes.

The FT-IR absorption spectrum is the preferred technique to identify the polymorphic forms of MBZ because they show characteristic differences in the shape and intensity of the major absorption bands at  $3370\text{ cm}^{-1}$  for the -NH- group and at  $1730\text{ cm}^{-1}$  for the -C=O group.<sup>20,24)</sup> In addition, a characteristic strong absorption band at  $1650\text{ cm}^{-1}$  from the -CNH- group can be also used. The values obtained in this work are similar to those reported for polymorph A (Table 2).

**Solubility Profiles** Tables 3 and 4 list the experimental solubility of MTZ, TBZ and MBZ. Figures 5—7 compare the solubility profiles of the drugs at 15—35  $^{\circ}\text{C}$  against the solubility parameter  $\delta_1$  of the solvent blends (Table 3). MBZ and MTZ show “chameleonic” behaviour, characterized by the appearance of two maxima at two distinct (higher and lower) polarity values whereas TBZ displays a single peak. The solubility of MTZ increases to reach a maximum at 80% v/v ethanol in water ( $\delta_1=30.8\text{ MPa}^{1/2}$ ), decreasing at higher ethanol concentrations. Lowering the polarity of the medium enhances the MTZ solubility to a second maximum at 50% v/v ethanol in ethyl acetate ( $\delta_1=22.5\text{ MPa}^{1/2}$ ). The presence of two peaks indicates that besides polarity the nature of the mixture (aqueous or non aqueous) determine solubility changes. MBZ also display two maxima at high and low polarity values: 80—95% ethanol in water ( $\delta_1=30.8\text{—}27.6\text{ MPa}^{1/2}$ ) and 60% ethyl acetate in ethanol ( $\delta_1=21.7\text{ MPa}^{1/2}$ ). A shoulder instead of a peak is observed for TBZ in ethanol-

Table 3. Solubility Parameters of the Solvent Mixtures and Solubility Mole Fraction of Metronidazole (MTZ) and Thiabendazole (TBZ) at 25  $^{\circ}\text{C}$

Ethanol ratio	$\delta_1$	$\delta_{1a}$	$\delta_{1b}$	$X_2$ (MTZ)	$X_2$ (TBZ)
Water-ethanol					
0	47.86	13.7	65.46	0.00075	$3.54 \times 10^{-7}$
0.1	45.73	14.03	60.04	0.00108	$1.31 \times 10^{-6}$
0.2	43.59	14.36	54.62	0.00121	$3.35 \times 10^{-6}$
0.3	41.46	14.69	49.2	0.00193	$8.46 \times 10^{-6}$
0.4	39.32	15.01	43.77	0.00332	$2.21 \times 10^{-5}$
0.5	37.19	15.34	38.36	0.00510	$5.06 \times 10^{-5}$
0.6	35.05	15.67	32.93	0.00634	$9.11 \times 10^{-5}$
0.7	32.92	16	27.51	0.00742	0.00016
0.8	30.78	16.32	22.09	0.00810	0.00028
0.9	28.64	16.65	16.67	0.00698	0.00035
1	26.51	16.98	11.25	0.00442	0.00040
Ethanol-ethyl acetate					
0.9	25.71	16.37	10.51	0.00505	0.00045
0.8	24.91	15.75	9.78	0.00632	0.00054
0.7	24.10	15.14	9.04	0.00715	0.00059
0.6	23.30	14.52	8.31	0.00776	0.00065
0.5	22.50	13.91	7.57	0.00874	0.00073
0.4	21.70	13.3	6.83	0.00791	0.00078
0.3	20.91	12.68	6.1	0.00708	0.00063
0.2	20.09	12.07	5.36	0.00622	0.00052
0.1	19.29	11.45	4.63	0.00480	0.00048
0	18.49	10.84	3.89	0.00310	0.00022

water at  $\delta_1=26.5\text{ MPa}^{1/2}$ . This drug shows a single and sharp peak at 40% ethanol-in ethyl acetate ( $\delta_1=21.7\text{ MPa}^{1/2}$ ).

Solubility profiles displaying one or two maxima have been reported for drugs within the polarity range covered by ethanol-water and ethanol-ethyl acetate mixtures. Curves with two maxima were found for more polar drugs with higher solubility parameter values such as caffeine and paracetamol.<sup>5,13)</sup> Solubility profiles with a single peak (usually in ethanol-ethyl acetate) were related to less polar drugs with lower solubility parameters as benzocaine.<sup>14)</sup>

**Relationships of Drug Solubility Parameter and Co-solvent Action** The experimental solubility parameter of a drug  $\delta_2$  can be determined from the Lin and Nash method,<sup>25)</sup> using the solubility mole fraction of the drug  $X_{2i}$  in three or five pure solvents of known solubility parameters  $\delta_{1i}$ :

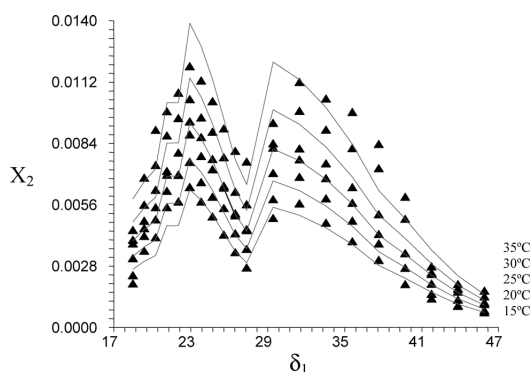
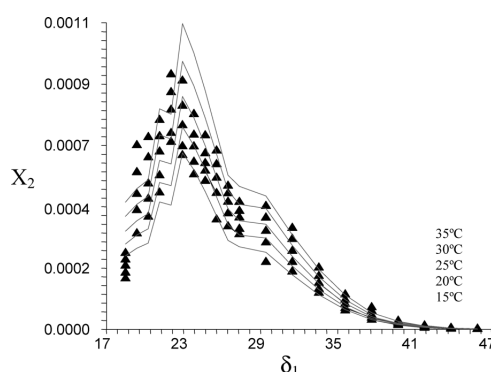
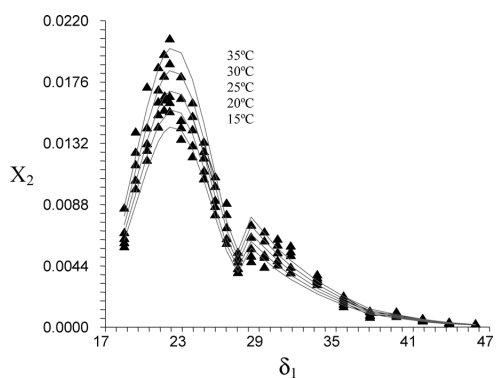
$$\delta_2 = \frac{\sum (X_{2i} \delta_{1i})}{\sum X_{2i}} \quad (2)$$

Table 4. Experimental Solubility of MBZ in Aqueous and Non-aqueous Mixtures at Several Temperatures

K	Ethanol : water (v/v)										
	0 : 100	10 : 90	20 : 80	30 : 70	40 : 60	50 : 50	60 : 40	70 : 30	80 : 20	90 : 10	100 : 0
308	0.0001	0.0002	0.0003	0.0005	0.0010	0.0010	0.0021	0.0037	0.0057	0.0067	0.0053
303	0.0001	0.0002	0.0003	0.0004	0.0009	0.0010	0.0019	0.0034	0.0053	0.0061	0.0049
298	$9.55 \times 10^{-5}$	0.0002	0.0003	0.0004	0.0008	0.0008	0.0017	0.0033	0.0050	0.0051	0.0046
293	$8.89 \times 10^{-5}$	0.0001	0.0002	0.0004	0.0007	0.0007	0.0015	0.0032	0.0042	0.0049	0.0041
288	$7.90 \times 10^{-5}$	0.0001	0.0002	0.0003	0.0007	0.0006	0.0014	0.0030	0.0038	0.0042	0.0038

K	Ethanol : ethyl acetate (v/v)										
	100 : 0	90 : 10	80 : 20	70 : 30	60 : 40	50 : 50	40 : 60	30 : 70	20 : 80	10 : 90	0 : 100
308	0.0053	0.0088	0.0107	0.0132	0.0160	0.0179	0.0206	0.0185	0.0171	0.0139	0.0084
303	0.0049	0.0080	0.0100	0.0125	0.0150	0.0163	0.0188	0.0169	0.0142	0.0124	0.0067
298	0.0046	0.0070	0.0090	0.0120	0.0141	0.0147	0.0165	0.0161	0.0131	0.0116	0.0063
293	0.0041	0.0062	0.0086	0.0111	0.0129	0.0142	0.0160	0.0151	0.0126	0.0104	0.0060
288	0.0038	0.0059	0.0080	0.0105	0.0121	0.0134	0.0154	0.0143	0.0119	0.0098	0.0057

Fig. 5. Solubility of Metronidazole in Ethanol–Water ( $\delta_1=26.51$ – $47.97 \text{ MPa}^{1/2}$ ) and Ethanol–Ethyl Acetate ( $\delta_1=26.51$ – $18.49 \text{ MPa}^{1/2}$ ) at 5– $35^\circ\text{C}$ Experimental ( $\blacktriangle$ ); calculated (solid lines, Eq. 3).Fig. 7. Solubility of Thiabendazole in Ethanol–Water ( $\delta_1=26.51$ – $47.97 \text{ MPa}^{1/2}$ ) and Ethanol–Ethyl Acetate ( $\delta_1=26.51$ – $18.49 \text{ MPa}^{1/2}$ ) at 15– $35^\circ\text{C}$ Experimental ( $\blacktriangle$ ); calculated (solid lines, Eq. 5).Fig. 6. Solubility of Mebendazole in Ethanol–Water ( $\delta_1=26.51$ – $47.97 \text{ MPa}^{1/2}$ ) and Ethanol–Ethyl Acetate ( $\delta_1=26.51$ – $18.49 \text{ MPa}^{1/2}$ ) at 15– $35^\circ\text{C}$ Experimental ( $\blacktriangle$ ); calculated (solid lines, Eq. 4).

Water, ethanol and ethyl acetate were used here (Table 5). The values of  $\delta_2$  calculated from the Fedors group contribution method<sup>26)</sup> are higher (Table 5) and nearer the solubility peak found in the more polar mixture (ethanol–water). The experimental values are closer to the peak obtained in the less polar mixture (ethanol–ethyl acetate). Although the solubility parameter values are different, both methods provide the same decreasing polarity trend for the drugs:  $\text{MTZ} > \text{TBZ} > \text{MBZ}$ .

Table 5 compares the maximum solubility enhancement relative to water ( $X_1^M/X_W$  and  $X_2^M/X_W$ ) and the ratio of the peak height in both mixtures ( $X_1^M/X_2^M$ ). The non-aqueous blend (ethanol–ethyl acetate) produces larger solubility increases for all co-solvent ratios and temperatures (15– $35^\circ\text{C}$ ). The solubility peaks of the most polar drug (MTZ,  $\delta_2=32.31 \text{ MPa}^{1/2}$ ) are of similar magnitude showing a similar co-solvent action for both mixtures (at the peaks the molar solubilities are  $0.0081 \text{ mol/l}$  and  $0.0079 \text{ mol/l}$  at  $25^\circ\text{C}$ ). For TBZ and MBZ the solubility peak in the non-aqueous mixture is much higher (Table 5).

The solubility enhancement varies with temperature in both mixtures and it is inversely related to the water solubility of the drugs:  $\text{TBZ} > \text{MBZ} > \text{MTZ}$ .

The ratios of the peak height ( $X_1^M/X_2^M$ ) slightly increase with temperature. For the drugs showing two peaks (MTZ and MBZ) the solubility enhancement ratios in ethanol–ethyl acetate ( $X_1^M/X_W$ ) and in ethanol–water ( $X_2^M/X_W$ ) are similar or somewhat larger at the highest temperature. For the less polar compound showing a single peak (TBZ) the trend is the opposite; both ratios decrease as the temperature is raised.

**Solubility Prediction** Equation 1 is fitted to all the experimental data for each drug, including both mixtures (ethanol–water and ethanol–ethyl acetate) and all temperatures (Tables 3, 4). The data used for MTZ and TBZ at 15, 20, 30 and  $35^\circ\text{C}$  can be found elsewhere.<sup>21)</sup> The following

Table 5. Solubility Parameters of the Drugs, Ratio of the Peak Height ( $X_1^M/X_2^M$ ) and Solubility Increase ( $X_1^M/X_W$  and  $X_2^M/X_W$ ) in Ethanol–Ethyl Acetate (1) and Ethanol–Water (2) and at 15–35 °C

Drugs	$\delta_2^{a)}$	$\delta_2^{b)}$	$X_1^M/X_2^M$		$X_1^M/X_W$		$X_2^M/X_W$	
			35 °C	15 °C	35 °C	15 °C	35 °C	15 °C
MTZ	32.3	25.4	0.93	0.88	12.84	10.79	13.67	12.23
TBZ	28.7	24.0	<sup>c)</sup>	<sup>c)</sup>	953	1612	2328	3182
MBZ	28.0	23.6	0.35	0.30	68	59	193	196

a) Calculated from the Fedors method.<sup>26)</sup> b) Experimental value from the Lin and Nash method.<sup>25)</sup> c) No peak in ethanol–water.

equations are obtained:

Metronidazole:

$$\ln X_2 = -13.8908(\pm 0.5) + 0.6557(\pm 0.05)\delta_1 - 0.0167(\pm 0.001)\delta_1^2 + 0.0533(\pm 0.06)\delta_{1a} + 0.5349(\pm 0.08)\delta_{1b} - 0.0646(\pm 0.003)\delta_{1a}\delta_{1b} + 0.0396(\pm 0.002)T + 0.6296(\pm 0.1)I$$

$$r^2 = 0.962 \quad n = 105 \quad \text{RMSE} = 0.156 \quad (3)$$

Mebendazole:

$$\ln X_2 = -20.1931(\pm 0.6) + 0.9895(\pm 0.04)\delta_1 - 0.0272(\pm 0.001)\delta_1^2 + 0.3697(\pm 0.04)\delta_{1a} + 1.1565(\pm 0.06)\delta_{1b} - 0.0618(\pm 0.003)\delta_{1a}\delta_{1b} + 0.0165(\pm 0.002)T + 0.5208(\pm 0.06)I$$

$$r^2 = 0.999 \quad n = 120 \quad \text{RMSE} = 0.109 \quad (4)$$

Thiabendazole:

$$\ln X_2 = -16.5663(\pm 0.6) + 0.7224(\pm 0.06)\delta_1 - 0.0196(\pm 0.001)\delta_1^2 + 0.1039(\pm 0.07)\delta_{1a} + 0.4185(\pm 0.09)\delta_{1b} - 0.0195(\pm 0.004)\delta_{1a}\delta_{1b} + 2.8081(\pm 0.002)T + 0.2282(\pm 0.1)I$$

$$r^2 = 0.994 \quad n = 105 \quad \text{RMSE} = 0.182 \quad (5)$$

RMSE is the root mean squared error and  $n$  is the number of cases.

The high correlations obtained ( $r^2$  values are larger than 0.96) show that the model is able to fit a large number of cases ( $n > 100$  for each drug), including all temperatures and two solvent mixtures. All the regression coefficients are statistically significant and their positive or negative signs agree with those expected, allowing a physical interpretation of the model. The terms associated with solute–solvent interactions ( $\delta_1$ ,  $\delta_{1a}$  and  $\delta_{1b}$ ) are positive, increasing solubility. The terms representing solvent–solvent interactions ( $\delta_1^2$  and  $\delta_{1a}\delta_{1b}$ ) are negative, lowering solubility. The negative intercept is related to the contribution of the solid phase (the melting step) that decreases solubility.

Figures 5–7 show that the model is able to predict the different solubility profile shapes found experimentally, *i.e.*, curves with two symmetrical (MTZ) or asymmetrical (MBZ) maxima, and with a single peak and a shoulder (TBZ).

To further test the prediction ability of the model, Eq. 1 is fitted to a smaller number of data, and the training equation is then used to predict solubility at other temperatures and co-solvent ratios not used to fit the equation. Unlike regression, prediction does not involve any fit of the data providing a better evaluation of the model. The prediction coefficient  $p^2$  is strictly analogous to  $r^2$  and is obtained as follows<sup>15)</sup>:

$$p^2 = 1 - \frac{\sum (\ln X_2 - \ln X_{\text{calc}})^2}{\sum (\ln X_2 - \ln X_{\text{mean}})^2} \quad (6)$$

where  $\ln X_2$ ,  $\ln X_{\text{calc}}$  and  $\ln X_{\text{mean}}$  are the experimental, calculated and mean values, respectively. The training data in-

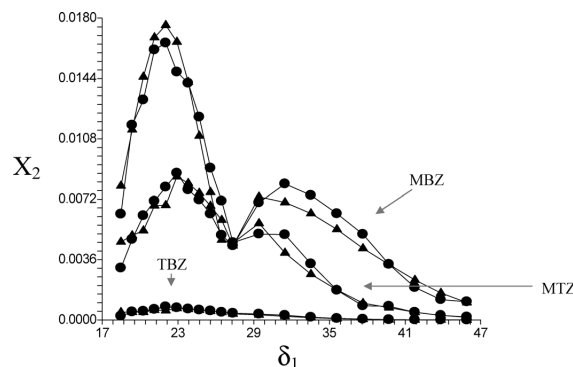


Fig. 8. Experimental (●) and Predicted (▲) Solubility for MTZ, MBZ and TBZ at 25 °C (Eq. 1)

cludes two temperatures (15, 35 °C) and the following co-solvent concentrations: 0, 30, 50, 70 and 90% ethanol in water and 10, 30, 50, 70 and 100% ethanol in ethyl acetate. The training equations are as follows:

Metronidazole:

$$\ln X_2 = -12.0894(\pm 4.52) + 0.6136(\pm 0.14)\delta_1 - 0.1199(\pm 0.005)\delta_1^2 + 0.1275(\pm 0.26)\delta_{1a} + 0.2336(\pm 0.36)\delta_{1b} - 0.1347(\pm 0.01)\delta_{1a}\delta_{1b} + 0.4274(\pm 0.003)T + 0.6561(\pm 0.21)I$$

$$r^2 = 0.973 \quad n = 120 \quad \text{RMSE} = 0.177 \quad (7)$$

Mebendazole:

$$\ln X_2 = -19.8604(\pm 2.7) + 0.8568(\pm 0.13)\delta_1 - 0.3047(\pm 0.006)\delta_1^2 + 0.6088(\pm 0.24)\delta_{1a} + 0.7146(\pm 0.38)\delta_{1b} - 1.4412(\pm 0.01)\delta_{1a}\delta_{1b} + 0.5629(\pm 0.003)T + 0.5234(\pm 0.16)I$$

$$r^2 = 0.995 \quad n = 120 \quad \text{RMSE} = 0.134 \quad (8)$$

Thiabendazole:

$$\ln X_2 = -13.5856(\pm 1.25) + 0.6417(\pm 0.12)\delta_1 - 0.364(\pm 0.004)\delta_1^2 + 0.1420(\pm 0.21)\delta_{1a} + 0.0062(\pm 0.29)\delta_{1b} - 0.0279(\pm 0.01)\delta_{1a}\delta_{1b} + 0.0441(\pm 0.003)T + 0.4891(\pm 0.17)I$$

$$r^2 = 0.997 \quad n = 105 \quad \text{RMSE} = 0.146 \quad (9)$$

All the regression coefficients are statistically significant and their values are comparable to those obtained with the whole data set (Eqs. 3–5). The positive and negative signs on the coefficients are also consistent with the model as found for the whole data set.

Equations 7–9 are used to predict the solubility at the remaining co-solvent ratios and temperatures. The prediction coefficients  $p^2$  (Eq. 6) are in general larger than 0.99 except for metronidazole at 20 °C. Equations 7–9 are able to predict different solubility profiles with one or two maxima using a limited number of data point, *i.e.* 20 data pair are used to predict more than 100 solubilities for each drug. Figure 8 shows a sample of the solubility profiles predicted at

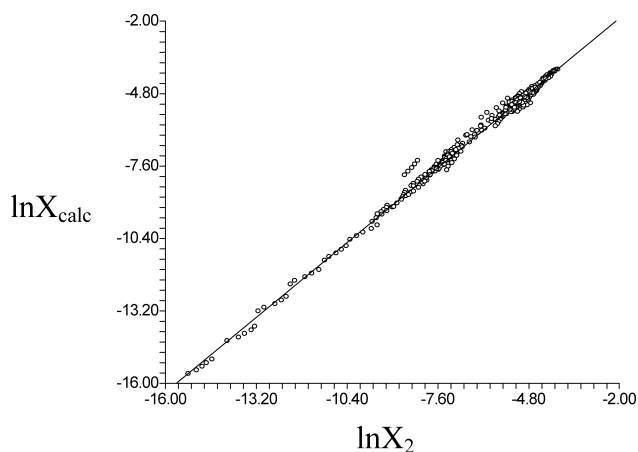


Fig. 9. Correlation between the Experimental  $\ln X_2$  and Predicted  $\ln X_{\text{calc}}$  Values (Eq. 1) for MBZ, TBZ and MTZ at All Temperatures

$$n=329; r^2=0.99.$$

25 °C for MTZ, and MBZ and TBZ. Figure 9 displays the correlation between the experimental and predicted solubility values (Eqs. 7—9) for all drugs at all temperatures ( $n=329$ ;  $r^2=0.99$ ).

### Conclusion

The single equation proposed here to model solubility curves with one or two maxima at several temperatures (Eq. 1) was able to reproduce the solubility profiles of all the drugs ( $r^2$  larger than 0.96). To our knowledge there is not other model that combines two mixtures and several temperatures in a single equation. The model showed true predictive capability because the solubility curves can be calculated at other temperatures and co-solvent ratios from a small data set (for each drug, more than 100 solubility values were predicted from 20 experimental data). The ability prediction is useful to save experiments that are often expensive and time consuming.

**Acknowledgements** The authors acknowledge the financial support of Ministerio de Ciencia y Tecnología (Project PM 99-0127).

### References

- 1) Jouyban A., *J. Pharm. Pharm. Sci.*, **11**, 32—58 (2008).
- 2) Pacheco D. P., Manrique Y. J., Martínez F., *Fluid Phase Equilbr.*, **262**, 23—31 (2007).
- 3) Bustamante C., Bustamante P., *J. Pharm. Sci.*, **85** 1109—1111 (1996).
- 4) Bustamante P., Romero S., Peña M. A., Escalera B., Reillo A., *J. Pharm. Sci.*, **87**, 1590—1596 (1998).
- 5) Bustamante P., Navarro J., Romero S., Escalera B., *J. Pharm. Sci.*, **91**, 874—883 (2002).
- 6) Peña M. A., Escalera B., Reillo A., Sánchez A. B., Bustamante P., *J. Pharm. Sci.*, **98**, 129—1135 (2009).
- 7) Nti-Gyabaah J., Chmielowski R., Chan V., Chiew Y. C., *Int. J. Pharm.*, **359**, 111—117 (2008).
- 8) Manrique J., Martínez F., *Lat. Am. J. Pharm.*, **26**, 344—354 (2008).
- 9) Gander B., Johansen P., Nam-Tran H., Merkle H. P., *Int. J. Pharm.*, **129**, 51—61 (1996).
- 10) Chen C., Crafts P. A., *Ind. Eng. Chem. Res.*, **45**, 4816—4824 (2006).
- 11) Mota F. L., Carneiro A. P., Queimada A. J., Pinho S. P., Macedo E. A., *Eur. J. Pharm. Sci.*, **37**, 499—507 (2009).
- 12) Machatha S. G., Bustamante P., Yalkowsky S. H., *Int. J. Pharm.*, **283**, 83—88 (2004).
- 13) Romero S., Reillo A., Escalera B., Bustamante P., *Chem. Pharm. Bull.*, **44**, 1061—1064 (1996).
- 14) Peña M. A., Reillo A., Escalera B., Bustamante P., *Int. J. Pharm.*, **321**, 155—161 (2006).
- 15) Bustamante P., Ochoa R., Reillo A., Escalera B., *Chem. Pharm. Bull.*, **42**, 1129—1133 (1994).
- 16) Escalera B., Bustamante P., Martin A., *J. Pharm. Pharmacol.*, **46**, 172—175 (1994).
- 17) Karger B. L., Snyder L. R., Eon C., *J. Chromatogr.*, **125**, 71—88 (1976).
- 18) Bustamante P., Escalera B., Martin A., Sellés E., *J. Pharm. Pharmacol.*, **45**, 253—257 (1993).
- 19) Agatonovic-Kustrin S., Glass B. D., Mangan M., Smithson J., *Int. J. Pharm.*, **361**, 245—250 (2008).
- 20) de Villiers M. M., Terblanche R. J., Liebenberg W., Swanepoel E., Dekker T. G., Song M., *J. Pharm. Biomed. Anal.*, **38**, 435—441 (2005).
- 21) Muela S., Escalera B., Peña M. A., Bustamante P., *Fluid Phase Equilbr.*, submitted (2009).
- 22) Rubino J. T., Blanchard J., Yalkowsky S. H., *J. Parenter. Sci. Technol.*, **41**, 172—176 (1987).
- 23) Himmelreich M., Rawson B. J., Watson T. R., *Aus. J. Pharm. Sci.*, **6**, 123—125 (1977).
- 24) Swanepoel E., Liebenberg W., de Villiers M. M., *Eur. J. Pharm. Biopharm.*, **55**, 345—349 (2003).
- 25) Lin H., Nash R. A., *J. Pharm. Sci.*, **82**, 1018—1026 (1993).
- 26) Fedors R. F., *Polym. Eng. Sci.*, **14**, 147—154 (1974).